International Journal of Naval Architecture and Ocean Engineering 15 (2023) 100549

Contents lists available at ScienceDirect

International Journal of Naval Architecture and Ocean Engineering

journal homepage: www.journals.elsevier.com/international-journal-of-naval-architecture-and-ocean-engineering/

Parameter space exploration for the probabilistic damage stability method for dry cargo ships

Bas Milatz [a,b], Roy de Winter [b,c], Jelle D.J. van de Ridder [b], Martijn van Engeland [d], Francesco Mauro [a], Austin A. Kana [a,*]

[a] Department of Maritime and Transport Technology, Faculty of Mechanical, Maritime and Materials Engineering, Delft University of Technology, Delft, the Netherlands
[b] C-Job Naval Architects, Hoofddorp, the Netherlands
[c] Leiden Institute of Advanced Computer Science, Leiden University, Leiden, the Netherlands
[d] DELFTship Maritime Software, Hoofddorp, the Netherlands

ARTICLE INFO

Keywords:
Damage stability
Multi-objective optimisation
Ship design
Parametric model
Global sensitivity analysis

ABSTRACT

The prediction of the statutory attained subdivision index is a challenging issue for the initial design of ships due to the design freedom offered by a probabilistic damage stability assessment. To this end, optimisation techniques integrated with a parametric model of the internal layout may generate a preliminary subdivision design, fulfilling damage stability regulations and cargo volume requirements. The present study explores using a multi-objective constrained optimisation algorithm coupled with a parametric model of a single hold cargo vessel, first investigating two design goal alternatives and secondly performing a global sensitivity analysis on the design variables for the most promising solution. The adoption, in parallel, of state-of-the-art practices shows the validity of the obtained solutions and the time benefits for designers. Nonetheless, the non-linear nature of probabilistic damage stability does not allow for clearly identifying the most impactful parameters on the attained survivability index.

1. Introduction

The ship design process synthesises multiple disciplines across naval architecture and marine engineering to realise a unique and complex product: the ship (Andrews and Dicks, 1997). The final result should reflect the best compromise solution between design attributes giving antithetic trends on multiple Key Performance Indicators (KPIs). Besides pure performances, there are statutory regulations to observe, limiting the design variables and, consequently, the final design efficiency and KPIs.

Among the multiple compliances required by regulatory agencies for the final design, damage stability is one of the most impactful for the design choices, influencing not only the main dimensions of the ship but also the internal arrangement. Furthermore, dealing with the modern probabilistic frameworks for the damage stability assessment (IMO, 2009, 2020b), the link between damage stability indicators and design variables is not straightforward (Koelman and Pinkster, 2003; Vassalos et al., 2007; Tuzcu, 2003). Some initial studies have been performed to derive fast surrogate models for damage stability in the early design stage but were limited to a select number of specific damaged areas (Naydenov and Georgiev, 2013) or oriented to new ship concepts pursuing a deterministic approach (Mauro et al., 2019).

A more accurate insight into the probabilistic problem needs a more advanced design stage, where an initial internal subdivision for the ship is available. In such a case, optimisation algorithms provide a valuable hint for investigating damage stability KPIs (Vassalos and Guarin, 2009). However, the focus of damage stability research and its implications for ship design have centred on passenger vessels (cruise ships and RoPax vessels), leaving cargo ships a bit aside. After the harmonisation process of damage stability performed during project HARDER (2000–2003), the principal effort in damage stability is understanding the flooding process to prevent and reduce the risk of loss of life. As such, the topic covers most passenger ships and has developed through a series of collaborative research projects like GOALDS (2009–2012), eSAFE (2017–2018) and finally, FLARE (2018–2022). During these projects, damage models (Lützen, 2014; Bulian et al., 2016), collision and

Peer review under responsibility of The Society of Naval Architects of Korea.
* Corresponding author.
E-mail addresses: basmilatz@hotmail.com (B. Milatz), F.Mauro@tudelft.nl (F. Mauro), A.A.Kana@tudelft.nl (A.A. Kana).

https://doi.org/10.1016/j.ijnaoe.2023.100549
Received 7 May 2023; Received in revised form 14 August 2023; Accepted 23 August 2023
Available online 7 September 2023

grounding dynamics (Conti et al., 2021; Zang et al., 2021), flooding tests (Ruponen et al., 2022), improvement of direct calculation tools (Spanos and Papanikolaou, 2014; Ruponen et al., 2019) and establishment of design-oriented damage stability frameworks (Papanikolaou et al., 2013; Bulian et al., 2019; Mauro et al., 2022, 2023) have been carried out mainly on passenger ships. Several publications thoroughly describe the most relevant enhancement to damage stability for passenger ships (Papanikolaou, 2007; Manderbacka et al., 2019; Vassalos, 2022; Vassalos et al., 2022b). The focus on passenger ships results in the definition of design guidelines for vessels having complex and fragmented internal layouts (Vassalos et al., 2022a; Krüger, 2023), which means the layouts investigated in the current research do not reflect the general arrangement of cargo ships. This paper argues that the constant growth in the last decades of the worldwide shipping fleet stresses the urgency of dedicating more effort to the damage stability of cargo ships in the design process.

Therefore, the contribution of this research is the creation of a framework for improving internal layout by means of an optimisation algorithm and sensitivity analysis, fulfilling the in-force damage stability requirements and potentially increasing ships' safety. The framework provides designers with an optimised initial reference for their projects. Instead of treating the probabilistic damage stability regulations as mere compliance standards, this framework enables designers to use them as a fundamental basis for the design process. The freedom and therefore advantages offered by this regulation can only be harnessed when it is taken into account from the very start of the design. A novel procedure is proposed, starting from a preliminary parametric model of the vessel, allowing for identifying the most suitable position of internal subdivision bulkheads to reach multiple goals while keeping the attained survivability index as damage stability KPI. Such a choice does not allow for using a defined analytical formulation for objective functions and constraints, resulting in a Black-Box Optimisation (BBO) problem (Alarie et al., 2021). The framework also employs the multi-objective optimisation algorithm SAMO-COBRA (de Winter et al., 2021, 2022) specifically designed to speed up the resolution of BBO problems.

The procedure is applied to a reference single large hold dry cargo ship, optimising the internal layout for maximum survivability through two distinct strategies: first, by looking at a configuration with the minimum amount of bulkheads sufficient to pass probabilistic regulations, and second, by considering the minimum number of bulkheads that approaches the maximum subdivision index and maximum cargo hold volume on the initial layout. The attained index reflects the ship's safety level, and the cargo hold volume represents the economic implications of the design. Ship design is a complex process that necessitates the consideration of numerous parameters and variables. By establishing a trend line that illustrates the correlation between safety level and economics, the designer can make more informed decisions.

Commencing with a design closely aligned with the required safety index, other design requirements can be addressed. While some adjustments may lead to a decrease in the attained safety index below the target, understanding the trends and correlations allows designers to efficiently increase the attained index without excessively compromising the cargo hold volume, ultimately avoiding sub-optimal designs.

The solution granting maximum survivability was the starting point for detailed global sensitivity analysis of the design parameters employing the Morris method (Morris, 1991). The results show the high non-linearity of the problem and the capability of the adopted procedure of exploring the design space with sufficient insight into the parameters influencing the survivability index. The obtained results are in line with manual processes used by designers, highlighting the advantages in terms of time and insight in the obtained damaged stability-oriented solution offered by the developed optimisation process.

2. Probabilistic Damage Stability (PDS) framework

Prior to discussing the optimisation strategy, a background on the key elements of the damage stability probabilistic framework is provided. The probabilistic approach to the damage stability assessment of dry cargo and passenger ships (IMO, 2020b) is based on the determination of an attained subdivision index (A-index), which needs to be larger than the required index (R-index) set by the same regulation. The A-index is the weighted sum of partial subdivision indices that are calculated for each ith loading condition:

$$A = \sum_{i=1}^{3} w_i A_i = 0.4A_{d_s} + 0.4Ad_p + 0.2Ad_l \tag{1}$$

$$A_i = \sum_{j=1}^{N_{dc}} p_j s_j \tag{2}$$

where w_i are the weight coefficients for the calculation draughts. The calculation draughts d_s (deepest), d_p (partial) and d_l (light) for the partial indices and their respective weights are defined by Regulation 2 (IMO, 2020b). In Eq. (2), p_j is the flooding probability for each of the N_{dc} compartments or group of compartments and s_j is the survivability metric associated with the jth damage case. This approach keeps the determination of p_j and s_j, generally called p- and s-factors, fully decoupled.

The present regulatory framework for damage stability, in SOLAS Ch. II-1 (IMO, 2020b), allows for determining the probability of flooding a compartment or a group of compartments by evaluating p-factors (and the corrections for penetration and vertical extents r- and v-factors) with specific analytic formulations valid to assess collision damage cases (SOLAS/II-1/B-1/7-1, SOLAS/II-1/B-1/7-2). These formulations result from the probabilistic distribution of SOLAS's damage characteristics, including their location. In particular, the p-factor refers to a longitudinal subdivision by watertight transverse bulkheads defining so-called "zones" (or watertight compartments). Therefore, the present SOLAS probabilistic approach is usually referred to as the "zonal" approach (Pawlowski, 2004). Such an approach enables fast calculation of p-, r- and v-factors thanks to the use of analytical formulae valid for collision damages.

However, this method requires a manual definition of the zones and necessitates intricate calculation of the flooding probabilities (by difference for multiple damaged compartments). Nonetheless, the analytic formulations of the zonal approach are exact only for box-shaped geometries; hence, they are approximations in the case of ship hulls. For such a reason, especially for complex ships like passenger vessels, p-factors are currently evaluated with an alternative approach, called "non-zonal" (Bulian et al., 2016), where damages derive from the sampling of damage dimensions from pertinent distributions (Mauro and Vassalos, 2022), abandoning the concept of "zones". Approaches similar to the "non-zonal" approach have been postulated also for shipping vessels like tankers (Krüger et al., 2008; Krüger and Dankowski, 2019), making the "non-zonal" way of thinking the way forward for damage stability assessment on ships.

On the other hand, the statutory assessment of s-factors is based on empirical formulations (see SOLAS Ch.II-1) derived from the static residual curve GZ for all the intermediate and final stages of flooding associated with the damage case. The s-factor formulations are all with values in [0, 1], thus the s-factors represent the probability to survive a specific event in a specific flooding condition, and could be categorised in the following three cases:

- $s = 0$: the vessel is statically capsized or with insufficient residual stability margin.
- $0 < s < 1$: the vessel has a reduced reserve of stability that may lead to capsize in case of additional loads.
- $s = 1$: the vessel has sufficient residual stability.

The resulting s-factor values combined with the associated p-factor lead to the determination of the attained survivability index A, as given

in Eq. (2). It is evident that such a formulation for the A-index cannot be reproduced with an analytic function, as the evaluation of s-factor requires the execution of ad-hoc hydrostatics calculations. Furthermore, by adopting the analytical formulations for p-in the "zonal" approach, the zoning process is difficult to handle analytically. Therefore, the inclusion of the A-index in an optimisation process as an objective function or constraints lead to the definition of a Black Box Optimisation (BBO) process, that will be discussed in the following sections.

3. Optimisation strategy

Optimising the subdivision of a ship (described in more detail in Section 5) by solely maximising the attained survivability index results in an unreasonably high A-index and in turn an unreasonably low cargo carrying capacity. Therefore, in order to optimise the survivability of the cargo ship while still maintaining an efficient design, an additional objective focused on the cargo hold volume is needed to include the workability of the ship in the optimisation process.

However, as discussed previously, the primary objective function, the A-index, is too complex to present analytically. Due to the scale and complexity of this calculation, a computer simulation is required to determine the eventual outcome of the objective function. When the objective function or the set of constraints are unknown, unexploitable, or even non-existent, the optimisation becomes what is known as a BBO (Alarie et al., 2021). The cargo hold volume is used as a second objective, which itself is not regarded as a BBO, as the volume can be calculated with low computational effort and with a limited amount of parameters. The objective functions are optimised with respect to a number of variables. Constraints are used to ensure logical conditions are satisfied during the optimisation. All parameters considered in this optimisation are continuous, which is an important characteristic of the optimisation method choice. Fig. 1 shows a flowchart of the proposed optimisation framework. As can be seen in the flowchart, the initial design together with the initial design parameters are used as input for both the sampling method and SAMO-COBRA algorithm (de Winter et al., 2021, 2022). These two methods iterate to a predetermined number of iterations. The goal of the parametric model is to generate the new design based on the input from one of the named methods and to generate the attained index as input for the SAMO-COBRA algorithm. The budget of the algorithm represents the pre-defined number of function evaluations of the algorithm. The budget is usually determined by performing a convergence study. Every parameter is defined by its

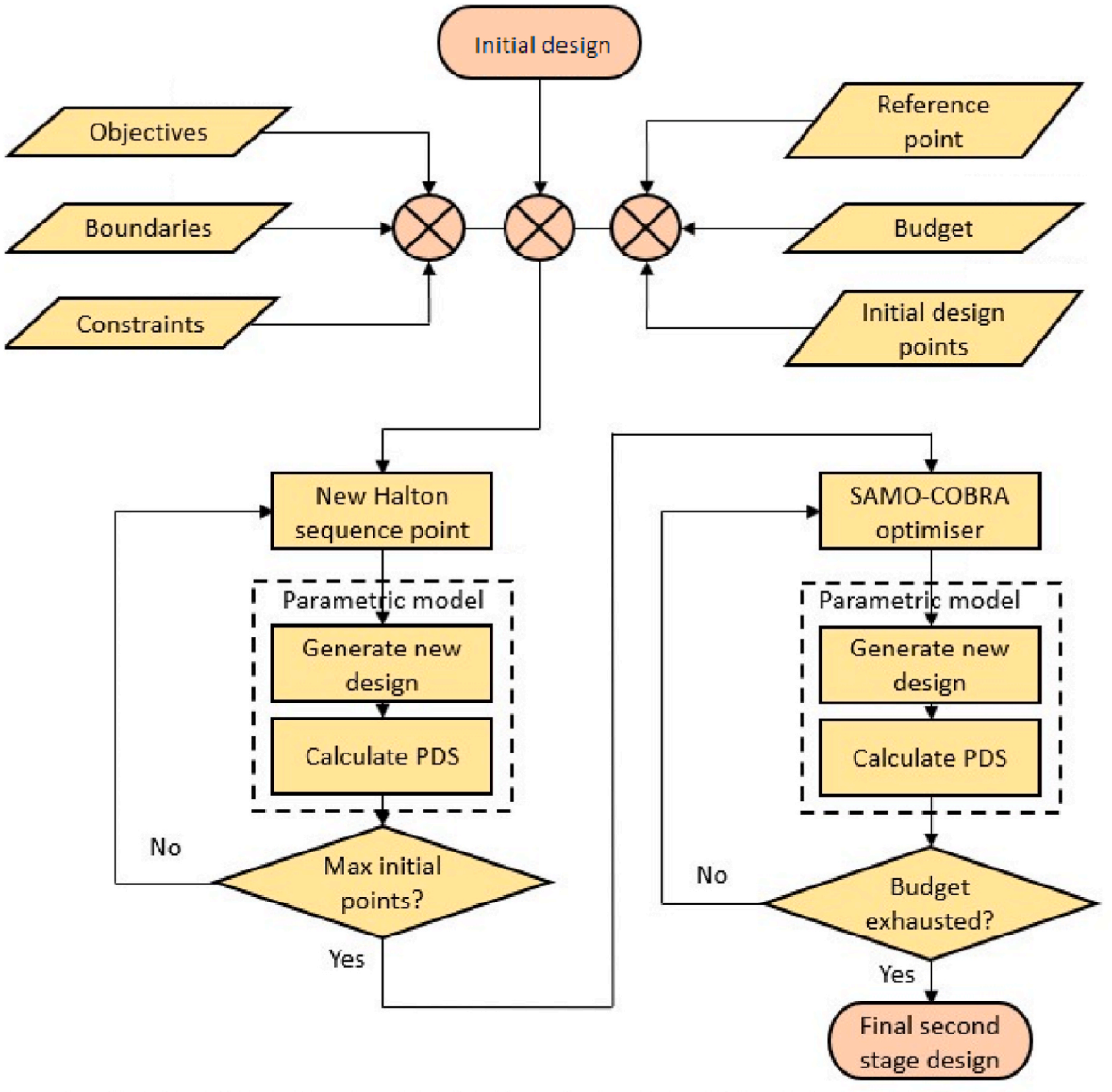

Fig. 1. Flowchart of the optimisation framework proposed.

boundaries. These boundaries represent the parameter range which the algorithm can use as infill points, where the infill points are the values given to the parameters by the algorithm that define the design of the model for that particular iteration.

The SAMO-COBRA algorithm is a self-adaptive algorithm for multi-objective constrained optimisation (de Winter et al., 2021, 2022). The algorithm consists of two phases. In Phase-I of SAMO-COBRA, the algorithm makes a first global estimate of the objective and constraint functions by learning from a starting set of variables determined with a design of experiments (DOE). In the DOE, a sampling method is used to choose well-spread solutions across the design space. SAMO-COBRA uses the Halton low-discrepancy sequence (Halton, 1960) which is proven by Bossek et al. (2020) to be an effective sampling method for BBO optimisation problems. The Halton sequence is fully deterministic in contrast to pseudo-random number sequences. It uses co-prime numbers as bases in each dimension to cover the design space uniformly. In total $3 \cdot d$ initial points are sampled where d is the number of decision variables. The $3 \cdot d$ initial points are used to train a surrogate model for each constraint and objective function. SAMO-COBRA uses Radial Basis Functions (RBFs) as a surrogate. RBFs exactly model the interaction between the decision variables and the constraint and objective values. This way, for all unseen decision variables values, the (computationally) cheap surrogates can be used to give a prediction for each constraint and objective function.

In Phase-II, SAMO-COBRA uses these cheap surrogates to find new optimal solutions. The COBYLA algorithm (Powell, 1994) is used to find the feasible optimal solutions. It does so by searching the optimum from a number of starting points towards a solution that is predicted by the surrogates to not violate any of the constraints while simultaneously scoring good in both objectives. To increase the chance of finding the global good solution, the number of starting points and the maximum number of COBYLA iterations can be increased. By increasing these two parameters, the calculation time of the algorithm increases as well. For the case study presented below, the calculation time per damage stability calculation is approximately 7 min, but can vary greatly with the complexity of the model and the type of hardware used. In this case a standard desktop PC was used with an Intel®Xeon ®CPU E3-1245 v3 processor, four cores and a clock speed of 3.40 GHz, with parallelisation. Thus, the time required for finding new infill points is therefore not considered to be very critical. When the algorithm can not find a new set of infill points where at least one of the constraints is satisfied, a warning is given and the solution with the smallest constraint violation is selected for evaluation in that particular iteration. After each iteration, the constraint and objective scores of the new solution are added to the archive which is used to train the surrogate models. This way, the accuracy of the surrogate improves every iteration which also lead to better infill points every iteration.

In order to find non-dominated solutions which form the Pareto front, the algorithm needs a reference point from where the hypervolume can be calculated. The hypervolume measures the volume of the dominated portion of the objective space Beume et al. (2007); Zitzler and Thiele (1998). This reference point consists of the least desired objectives scores possible for both objective functions. For the attained index, this is zero, meaning no damage cases add anything to the attained index. For the cargo hold, the minimum volume is dependent on the boundaries given to the respective parameters that influence the cargo hold volume.

The last step prior to optimising is to determine the amount of real function evaluations. Convergence for a multi-objective optimisation method like SAMO-COBRA is measured using the hypervolume progress (de Winter et al., 2021, 2022). With each new feasible Pareto efficient point, the Pareto front changes and the hypervolume is slightly increased. The highest possible hypervolume value is the area or volume between the reference point and all possible feasible non-dominated solutions. Convergence is reached when the hypervolume does not increase anymore or does so only marginally. To be confident that the optimisation algorithm is converged, a first experiment is performed with a large evaluation budget.

The SAMO-COBRA algorithm is defined as a minimisation algorithm. Hence, in the case an optimisation problem aims to maximise the objectives, the objective functions are transformed without the loss of generality as follows:

$$\max(f(x)) = \min(-f(x)) \tag{3}$$

To maximise both the attained index and the cargo hold volume, one can simply take the two functions in Eq. (4) as a BBO objective function, where A is the attained index returned from the hydrostatic calculations and V_{cargo} is the cargo hold volume derived from the internal layout.

$$\begin{aligned} Objectives: f_1(x) &= A \\ f_2(x) &= V_{cargo} \end{aligned} \tag{4}$$

The SAMO-COBRA algorithm considers all constraints as being equally important and feasible when the constraint score is below 0. This ensures a constraint violation by for example the cargo hold is not more important than the fuel tank, just because the constraint violation is larger in an absolute sense. This is reached by enforcing 0 as the feasibility boundary and by scaling every constraint output every algorithm iteration as follows:

$$c' = \frac{c}{\max(c) - \min(c)} \tag{5}$$

where:

c' = Normalised constraint scores;
c = All originally observed constraint scores so far;
$\max(c)$ = Maximum constraint score encountered so far;
$\min(c)$ = Minimum constraint score encountered so far.

This new approach is tested by employing a parametric model based on an reference design provided by C-Job Naval Architects.

4. The reference parametric ship model

The parametric model is built in the DELFTship software (DELFTship Maritime Software, 2022). The variable values, or infill points, proposed by the optimisation method are used as input for this model. The bulkheads, openings and decks that can be automatically modified by the variables are located in the middle section of the ship. The ship is divided into three parts, an aft, middle and forward section, whereby only the middle section is the focus of this research. The middle section is located between the aft and forward cargo hold bulkhead, as can be seen in Fig. 2. Although this could potentially impose some limitations on the results and insight of this research, it greatly reduces the number of design variables, eliminating the need for dimensionality reduction measures in that particular section, which in turn increases the insight in that section. This is vital for creating insight into how the single large hold reacts to different modifications. Also including the aft and forward sections of the ship results in a more holistic problem that could potentially lead to a wrong interpretation of how the variables react due to the high complexity of the model. It is still possible to shift the cargo hold in longitudinal direction in its entirety, this allows for changing the size and location of the sections.

Fig. 2 shows the base ship model that is used as the case study for this research. The main particulars of the ship are given in Table 1. These remain constant throughout the optimisation, as the goal of this research is to optimise the subdivision within the given ship's main dimensions.

The base ship is fully designed regarding the Probabilistic Damage Stability (PDS) calculations. Critical points such as openings, watertight doors, escape routes, deck lines and tank connections from the example ship are added to the base ship to try and create a realistic model that is suitable for this research. The model is flexible and generic to be

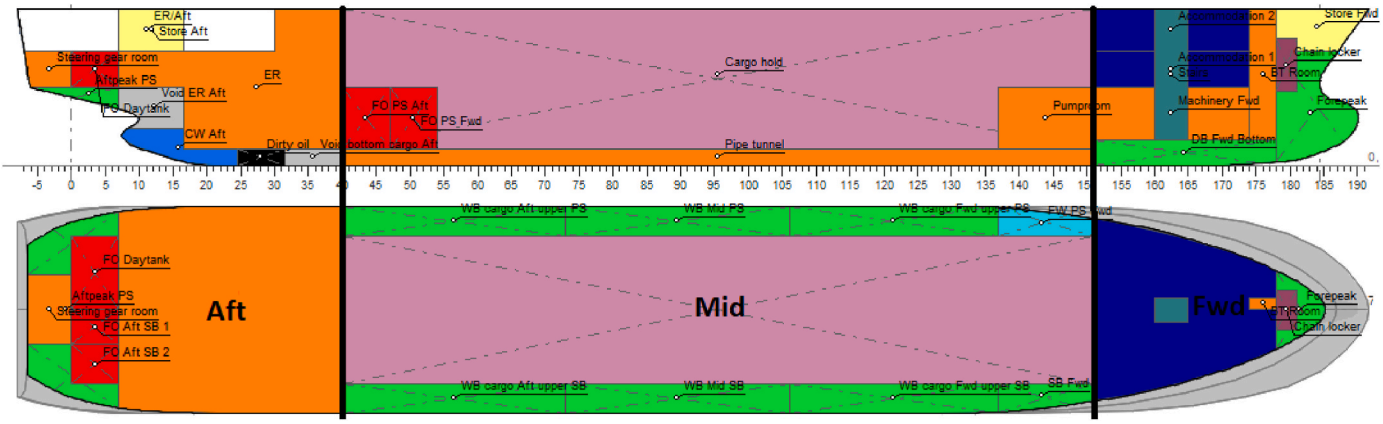

Fig. 2. Reference base ship model in the DELFTship environment with the various spaces labeled within the layout. Of particular note are the fuel oil tanks marked in red, and the pump room located at the front of the cargo hold.

Table 1
Main particulars hypothetical base ship model.

Parameter	Value
Ship type	General cargo ship
Subdivision length (L_s)	109.76 m
Length between perpendiculars (L_{PP})	101.42 m
Subdivision beam (B_s)	16.80 m
Moulded depth (D)	9.30 m
Light subdivision draught (d_l)	3.44 m
Partial subdivision draught (d_p)	4.94 m
Deepest subdivision draught (d_s)	5.94 m
Displacement (Δ)	7882.28 T

applicable to many different designs. Furthermore, it is detailed enough to cover all essential characteristics of the design, while simultaneously being as simple as possible to avoid unnecessary complexities. These goals are all reached, while also ensuring the model's integrity, robustness and functionality.

The DELFTship program uses the zonal concept to divide the parametric model into subdivision zones used in the PDS calculation. In such a case the zones are automatically generated as a function of tank boundaries. This comes in handy when subjecting the parametric model to an optimisation method. For every iteration, a new design is generated, hence needing a new zonal subdivision. Fig. 3 shows the zonal subdivision from the starboard side and from the top down view.

The infill points generated by the algorithm and sensitivity analysis are divided into three different types of variables: independent, dependent, and semi-independent. The location of the independent variables is the value that is returned as an infill point from the optimisation method. The location of the dependent variables are determined only by a fixed distance from another variable. The last type is the semi-independent variables, defined in Eq. (6). These have a fixed distance from another variable, where the infill point represents a delta value that scales the size of the compartment relative to the coupled plane.

$$x_{semi} = x_A + x_B + \Delta_C \tag{6}$$

where:

x_{semi} = Distance of the semi-dependent bulkhead from the origin;
x_A = Distance of the independent bulkhead from the origin;
x_B= Fixed distance from the independent bulkhead;
Δ_C= Independent component of the semi-dependent bulkhead.

The direction in which the parameter is shifted is added to the variables by means of a vector, defined in Eq. (7):

$$\mathbf{v}' = x_{semi-dependent} \cdot \begin{bmatrix} v_x \\ v_y \\ v_z \end{bmatrix} \tag{7}$$

where $v_{x,y,z}$ is the distance in their respective direction in the ship fixed coordinate system. The objectives, constraints, design parameters, and their abbreviations that comprise the middle section of the base ship are listed in Table 2.

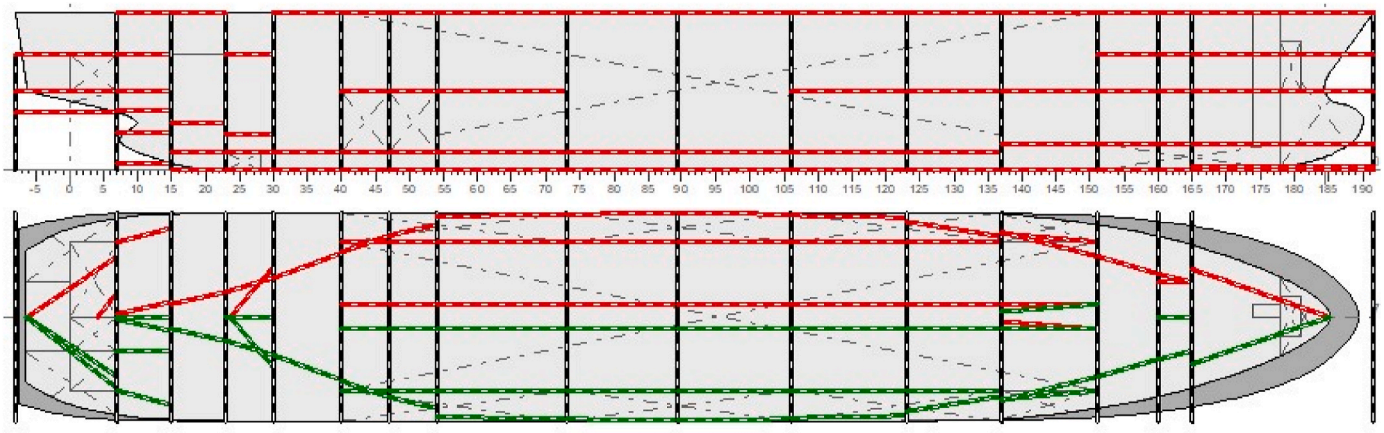

Fig. 3. Parametric model showing the subdivision (red, green and black lines) used for the PDS calculation. In top down view red and green lines differentiate port and starboard.

Table 2
Definition of all objectives, constraints, and design parameters with their respective abbreviations, where i is the index of the bulkhead.

	Objectives	Abbreviation
	Attained index	A
	Cargo hold volume	CH_{Vol}
	Constraints	
	Fuel oil tank volume	FO_{Vol}
	Required index	R
	Pump room volume	PR_{Vol}
	Longitudinal parameters	
1	Cargo hold aft bulkhead	CH_{Aft}
2	Cargo hold forward bulkhead	CH_{Fwd}
3	Fuel oil tank separation bulkhead	FO_1
4	Fuel oil tank forward bulkhead	FO_2
5	Pump room bulkhead	PR_{Trans}
	Transverse parameters	
6	Double hull	DH
7	Pipe tunnel	PT
8	Water ballast bulkhead	WB_i
	Vertical parameters	
9	Tanktop	TT
10	Tweendeck	TD
11	Main deck	MD
12	Fuel oil tanks	FO_{Vert}
13	Pump room	PR_{Vert}
14	Openings	O

5. Multi-target optimisation of the internal layout

As discussed in Section 3, two objective functions are used where both the survivability of the ship is optimised as well as the cargo hold volume. The boundaries are kept at the widest possible margin and the number of constraints are kept to a minimum in order to fully utilise the freedom of the algorithm. In other words, to explore as much of the parameter space as possible while maintaining a relatively high feasibility rate for the proposed designs. The objective functions and constraints used for this case study are the following:

$$\begin{aligned} \text{Objectives}: f_1 &= -A \\ f_2 &= -V_{cargo} \\ \text{Constraints}: g_1 &\leftarrow V_{FO\ aft\ min} - V_{FO\ aft\ actual} \leq 0 \\ g_2 &\leftarrow V_{FO\ fwd\ min} - V_{FO\ fwd\ actual} \leq 0 \\ g_3 &\leftarrow V_{PR\ min} - V_{PR\ actual} \leq 0 \\ g_4 &\leftarrow R - A \leq 0 \end{aligned} \tag{8}$$

Three geometrical inequality constraints are used to compare the minimum required volume of the fuel oil tanks (V_{FO}) and pump room (V_{PR}) against the actual volume from the model, preventing infeasible solutions as a result of infeasible compartment sizes. The last constraint ensures that the attained index is always higher than the required index, as all designs that have a lower attained index than required are considered not feasible by the PDS regulations. In Eq. (8), the constraints are written such that a negative value satisfies the constraint.

The number of transverse bulkheads used in the middle section of the ship is determined by looking at the minimum number necessary to satisfy the required index, using the base ship model. Also the number of bulkheads just before convergence is taken as a second design to see the difference between these two designs. Fig. 4 shows the results of the first optimisation level. As the position of the bulkheads is equally divided over the cargo hold length, they are not located in their optimum position in the first stage. Investigation showed that when changing the bulkhead location a slightly more favourable result can be obtained and the graph follows close to the corrected results line. Two and five bulkheads are chosen as possible number of bulkheads for this study, where two is the first number of bulkheads that satisfies the required

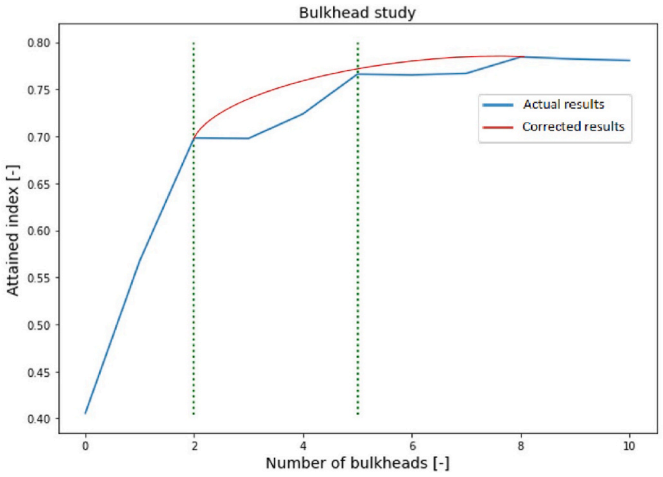

Fig. 4. Results from the first optimisation level.

Table 3
Comparison between two and five bulkheads in the ballast water tanks.

	Advantages	Disadvantages
Two BH	Low added weight	Less ballast freedom
	Lower construction costs	Lower A-Index
	Less exstensive ballast system	Lower stiffness
Five BH	Higher A-Index	More added weight
	More ballast freedom	Higher construction costs
	Higher stiffness	More extensive ballast system

index (R) with some margin. The definitive number of bulkheads is determined on more than the attained index only. Table 3 shows the considerations that can be made besides the results from the optimisation when choosing a number of bulkheads. The two and five bulkhead designs are chosen based on these considerations.

As mentioned in Section 3, the amount of real function evaluations is first determined, which can be seen in Fig. 5. To be confident that the optimisation algorithm has converged, a first experiment is performed with a large evaluation budget. For both the two and five water ballast bulkhead designs, suitable convergence was reached after about 200 iterations over 36 h with a minimum of 15 Pareto efficient points.

The extremities of the Pareto front were used to identify the behaviour of the PDS calculation. The design with the lowest attained index and highest cargo hold volume as well as the design with the highest attained index and lowest cargo hold volume is compared to

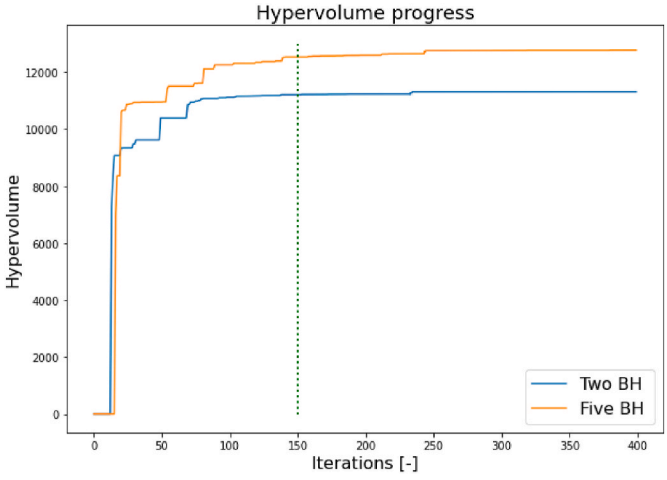

Fig. 5. Hypervolume progress for 400 iterations and both the two and five water ballast bulkhead design.

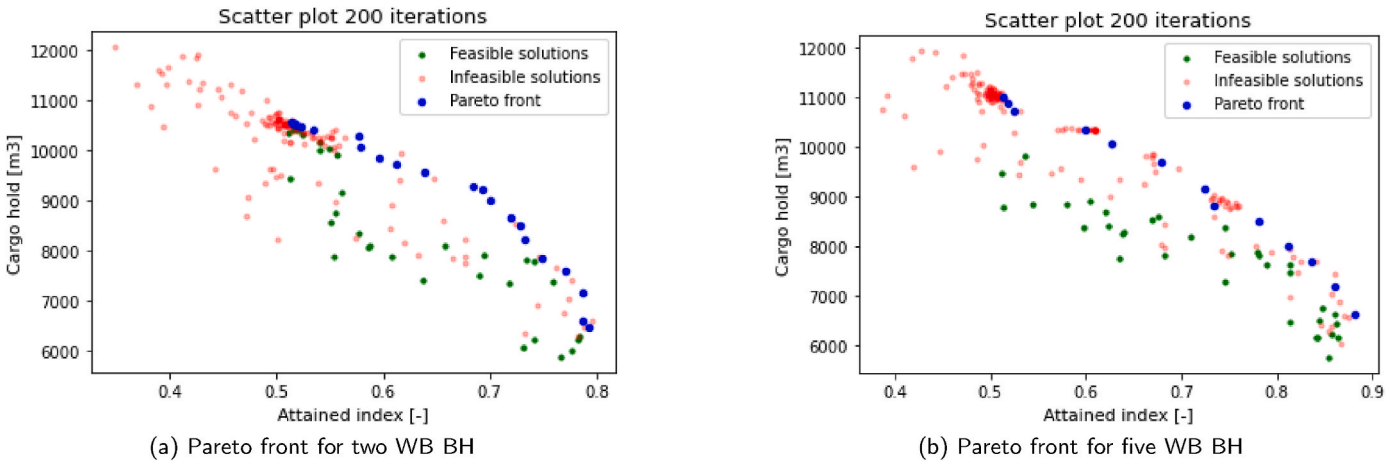

Fig. 6. Scatter plots of the Pareto fronts for two and five water ballast bulkheads (WB BH) investigated designs for 200 iterations.

explain the decisions of the algorithm for every design on the Pareto front. 22 initial design variations are found, enough to form a sufficient Pareto front. The resulting Pareto front for two water ballast bulkheads is shown later in this section in Fig. 6(a).

Likewise, Fig. 6(b) shows the behaviour of the parameter locations over the entire objective range for five water ballast bulkheads. The aft and forward bulkhead of the cargo hold do not show the same behaviour as can be seen in Fig. 12(a) and (b). These bulkheads both influence the size of the cargo hold equally and determine the size of the aft and forward sections of the ship. There is however, one significant difference regarding the influence on the subdivision of these two parameters. As the forward section of the ship is slimmer than the aft section, the position of the forward bulkhead greatly influences the distance of the cargo hold to the side shell of the ship, influencing the chance of penetration of the cargo hold significantly more than the aft bulkhead. Figs. 2 and 3 show this more clearly, where the forward bulkhead lies closer to the start of the parallel mid-body compared to the aft bulkhead, which still has some distance it can move aft before the outer hull becomes slimmer. The distance of the outer hull to the cargo hold influences the chance a damage penetrates the cargo hold.

5.1. First results analysis

In both extremities of the Pareto front (lowest attained index and highest cargo hold volume and vice versa), the aft FO tanks are not located fully on the inside of the double hull. In between these extremities the FO tanks also never reach the inside of the double hull. This is later also confirmed in Figs. 16 and 17, where the double hull and cargo hold aft parameter follow a linear line which gives this same result. The FO tanks are relatively small, compared to the cargo hold. They form a barrier between the cargo hold and the side shell. A penetration of the FO tanks instead of the cargo hold results in less loss of buoyancy and is therefore used as a barrier. Regarding the possibility of FO tanks to be located against the outer hull, regulation 12A is only applicable to ships with an aggregate FO capacity of $600m^3$ and above (MARPOL - International Convention for the Prevention of Pollution from Ships, 2007). The pump room also has this same behaviour regarding the protection of the cargo hold. Fig. 7 shows a visualization of the pump room in the cargo hold, where 1 is the pump room, 2 is the double hull water ballast tank, and 3 is the hull that now makes up the boundary of the cargo hold.

The tanktop is at its minimum height for every single point on the Pareto front. The reason for this is that the tanktop is located below the light subdivision draught in its entire range. This means that the PDS calculation always assumes that everything below the tanktop does not add any buoyancy (as they will be flooded in any subdivision draught

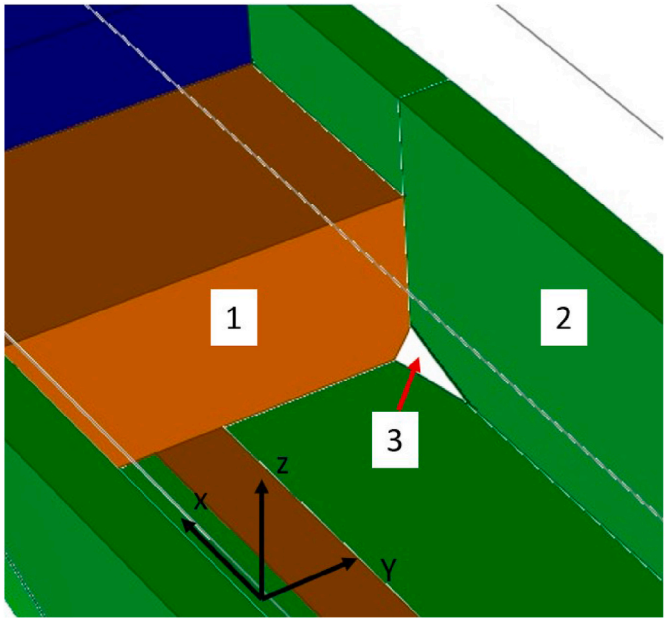

Fig. 7. Visualization of the pump room within the cargo hold, showing the part of the double hull that can be "protected" by moving the pump room bulkhead more to the aft. 1 is the pump room against the forward cargo hold bulkhead, 2 is the double hull water ballast tank, and 3 is the hull that now makes up the boundary of the cargo hold.

and therefore not contributing to the attained index). All compartments above the tanktop have volumes that are located above one of the waterlines. Therefore, if the tanktop height increases, the tanks located above it have less volume and are therefore adding less buoyancy, resulting in a lower attained index. The tanktop is therefore not adding any attained index and therefore always located at its minimum height. Because of this, a minimum height of the double bottom is given by SOLAS chapter II-1 part B-2 regulation 9 (IMO, 2020a) of $h = B/20$ where B is the breadth of the ship.

The maximum heeling angle for cargo ships is 30°, with an additional 16° as the maximum range of positive righting levers (IMO, 2020a). Openings that are designed to extend beyond this maximum heeling angle do not contribute to the attained index. Fig. 8 shows the damaged waterline for this PDS calculation and the openings at their lowest allowed value. The starboard openings are located below the waterline at this point. When the openings are located approximately 60 cm higher, they do not contribute to a higher attained index. Note that this

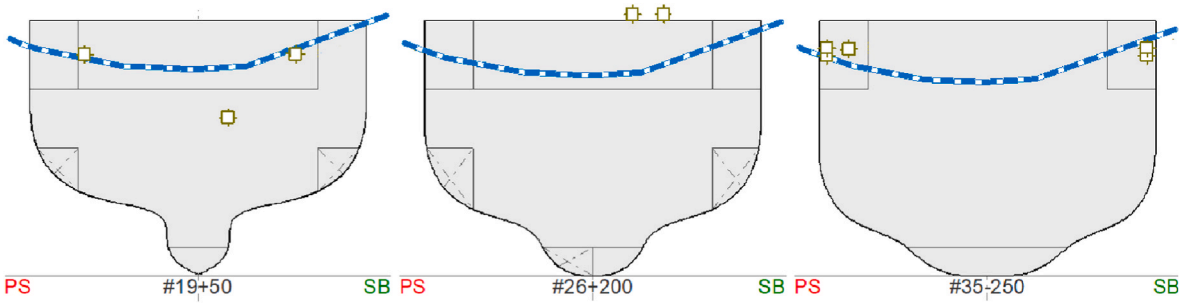

Fig. 8. Damaged waterline (blue/white line) and location of openings (squares) at position zero for different cross sections.

distance only counts for the base ship as the openings are changed relative to the main deck. This means that for the full influence of the openings the total variables space should be investigated by means of a global sensitivity analysis or a similar method.

5.2. Pareto-front extremity analysis

Fig. 9 shows the Pareto frontiers for both bulkhead configurations, highlighting the extremities of the optimal solutions.

Figs. 10 and 11 show the designs corresponding with the extremities of both Pareto fronts. Designs A and C have the lowest possible attained index, whereas designs B and D have the highest possible attained index for its respective amount of bulkheads. What becomes apparent is that most of the decisions by the algorithm with respect to increasing the attained index can be linked to the increase in distance from the cargo hold to the hull. The following phenomena are related to that cause:

- The position of the forward cargo hold is much more critical as it has more impact on the distance between the cargo hold and the hull than the aft bulkhead;
- The pump room is used as a sort of crumple zone between the cargo hold and the hull;
- The FO tanks are also used for this purpose;
- The volume of the double hull has a strong positive correlation with the attained index.

Only the openings, main deck and the height of the tanktop are not related to the protection of the cargo hold. The openings stop contributing to the attained index after a certain height and the tanktop is kept at a minimum due to the increase in buoyancy of compartments that are (partially) located above the waterline.

What can be concluded is that for the lower attained index regions (approximately up till 0.65), no increase can be seen in both attained index and cargo hold volume between the two and five bulkhead design. The small improvement shown is significantly less than in the higher attained index region. The double hull variable is measured from the centreline of the ship to the longitudinal cargo hold bulkhead, where the shape of the outer hull remains constant. Following the double hull trend lines from the parallel coordinate plots in Fig. 12(a) and (b), it can be concluded that the size of the water ballast tank in the side shell has a strong positive correlation with the attained index.

In the context of small side shell water ballast tanks, the contribution of buoyancy to the overall design is relatively insignificant. As a result, the distinction between two different designs is minimal at this scale. However, as the size of the side shell tanks increases, a considerable amount of buoyancy is introduced into the design. Consequently, when multiple bulkheads are incorporated within this enlarged buoyancy area, the attained index experiences a more substantial variation.

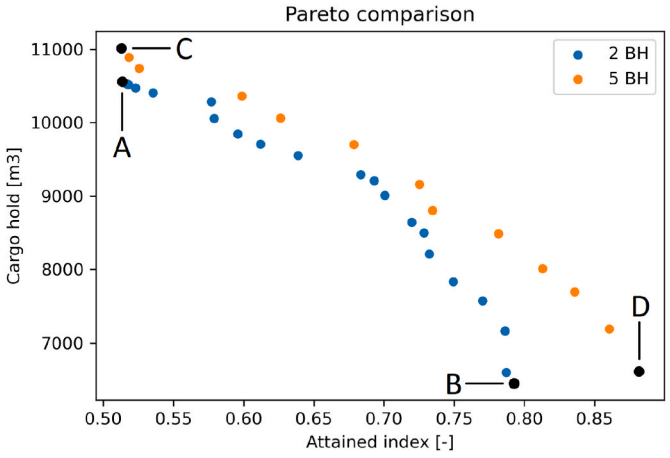

Fig. 9. Comparison of the Pareto front for the two respective bulkhead configurations.

6. Sensitivity analysis

Three sensitivity analysis methods were performed to create more insight in the decisions that can be made to further increase the attained index. The methods were the Morris method (Morris, 1991), the Pearson correlation matrix (Pearson, 1896), and a manual local analysis.

6.1. Morris method

To compute the Morris indices, the SALib package was used (Herman and Usher, 2017). The number of trajectories[1] the Morris method uses is defined by N. The total number of function evaluations is $N\ (p_s + 1)$, where p_s is the dimension of the parameter space, which was 16 for this case study. The Morris method uses few function evaluations compared to other sensitivity analysis methods. Typically, the elementary effects method such as the Morris method uses 10 to 50 trajectories in the input space (Campolongo et al., 2007). Approximately 50–60 trajectories are required according to Campolongo et al. (2005) and Herman et al. (2013), who compare the results of both the Sobol and Morris methods for different sample (trajectory) values. They show that there is little benefit from using a sample size N greater than 20. Their study was performed that looked at the number of trajectories between 20 and 100 with an interval of 20 for 14 parameters. If less than 10% of the sensitivity index value for the most sensitive parameter is represented for a confidence interval of 95%, convergence was considered acceptable. As this case study uses only two more parameters, a similar strategy is used to determine the right number of trajectories for this research. Three separate model runs were performed with 20, 60 and 100 trajectories respectively with the same confidence interval. To illustrate, the confidence interval is defined in Eq. (9), where μ is the mean of the elementary effects and μ^* is the mean of the absolute values of the

[1] The succession of points in which two consecutive elements only differ for one parameter, starting from a random base vector.

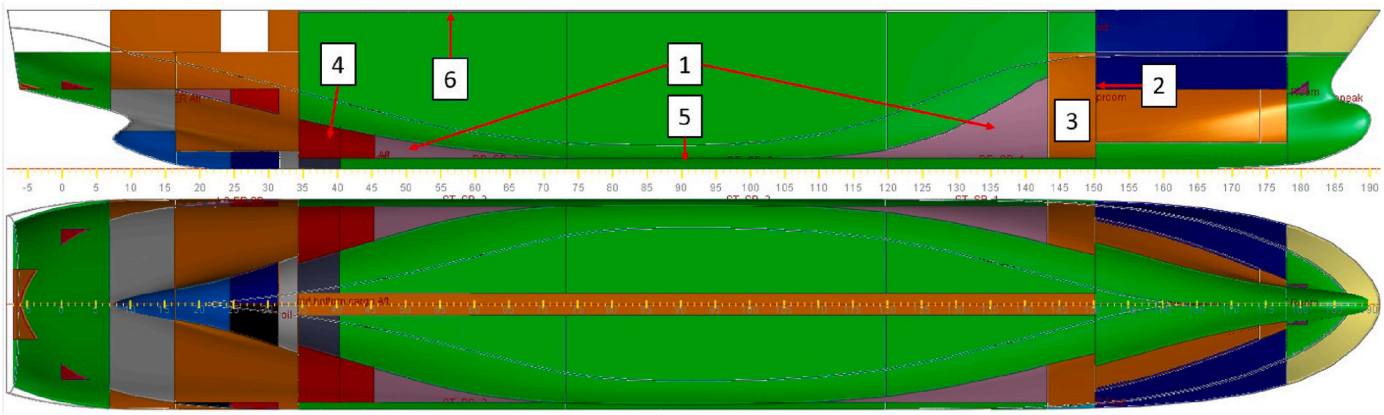

(a) Lowest Attained index of 0.513 with a corresponding cargo hold volume of 10,552 m^3. Notable properties of the design include: (1) cargo hold is not located within the double bottom, (2) forward cargo hold bulkhead is shifted towards the bow, (3) pump room is at its maximum height and minimum length, (4) fuel oil tanks are higher and more located to the aft, (5) double bottom is at its minimum height, and (6) main deck is at its maximum height.

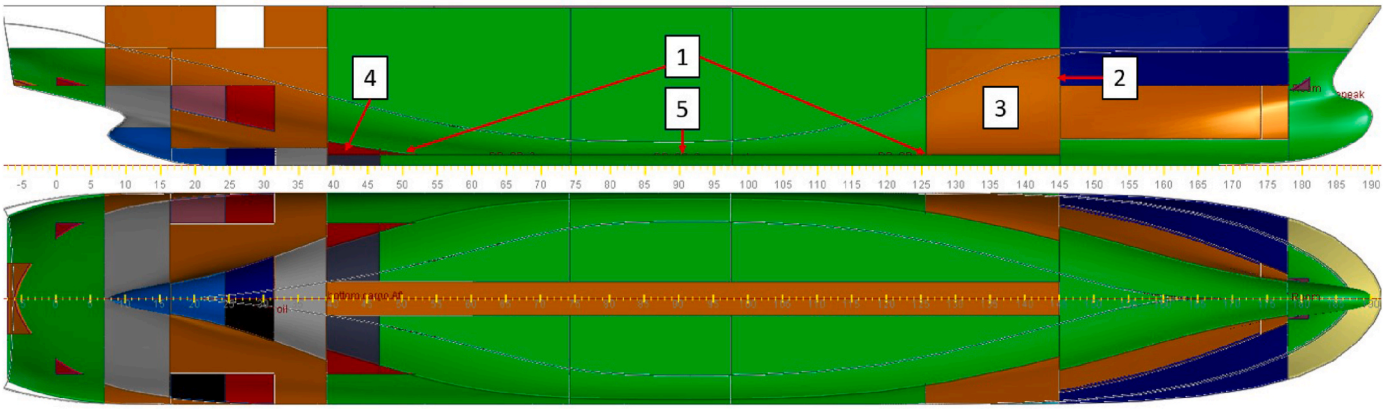

(b) Highest Attained index of 0.792 with a corresponding cargo hold volume of 6,453 m^3. Notable properties of the design include: (1) cargo hold is located inside double hull by a considerable margin, (2) forward cargo hold bulkheads shifted towards aft, creating the largest possible volume, (3) pump room bulkhead shifted towards aft, (4) fuel oil tanks not located inside double hull, and (5) double bottom stayed its minimum height.

Fig. 10. Extremities of the Pareto front for two water ballast bulkheads.

elementary effects:

$$10 > \frac{100 \cdot \mu^*}{\mu} \tag{9}$$

Each variable range is broken up into a grid by the Morris sampling method, considering an even number of threshold values higher or equal to four. In case the minimum value of four is chosen, the following quantiles of the factor distribution are taken: 12.5th, 37.5th, 62.5th and 87.5th (Saltelli et al., 2004). Campolongo and Saltelli (1997); Campolongo et al. (1999, 2007) demonstrated that the choice for four grid levels has produced valuable results and is therefore also used for this case study.

The resulting parameter sets for the trajectory values of 20, 60 and 100, result in 320, 1020 and 1600 sets respectively. These are then fit for being run through the parametric model. The same model as was used for the optimisation is used for generating the required output. The only difference being the input and output file handling to fit them into the Morris method. To calculate the Morris indices, the parameter file, the output file, and the number of objectives is required. For the optimisation, a multi-objective approach was used, which included the volume of the cargo hold. This objective is not interesting for the sensitivity analysis, as it is trivial what parameters influence it the most, namely the parameters that represent the main dimensions of the cargo hold.

Finally, the mean and variance of each parameter's elementary effects, given by μ and σ respectively, can be interpreted. The mean of the absolute values of the elementary effects is given by μ^* and is the best approximation of the "total" sensitivity (Herman and Usher, 2017). Fig. 13 shows the outcome of determining the number of trajectories. For $N = 20$ iterations, where the confidence interval is already below the 10% threshold, namely 8.56%. The number of iterations used for this analysis is therefore 1020.

Fig. 14 shows both the elementary effect as well as the standard deviation that makes up the bootstrap confidence interval in two ways. The first is the same as is shown in Fig. 13 and provides a quick overview of the most influential parameters. The second figure aims to indicate if the parameter behaves linear, non-linear, monotonic or non-monotonic. Almost all parameters, except the top three, are located on the line of non-linearity and non-monotonic. The confidence bootstrap interval is approximately 8.1% of the total elementary effect of the double hull parameter. This is, again, within the limit and confirms that 20 trajectories is good enough for this case study. However, a parameter like the openings shows that the confidence interval is more than 100% of the absolute value for the elementary effects regarding that specific parameter. For the next couple of parameters in the vicinity of openings, this lays around 50%, which is still considered as unreliable. This number decreases the higher the elementary effect per parameter goes,

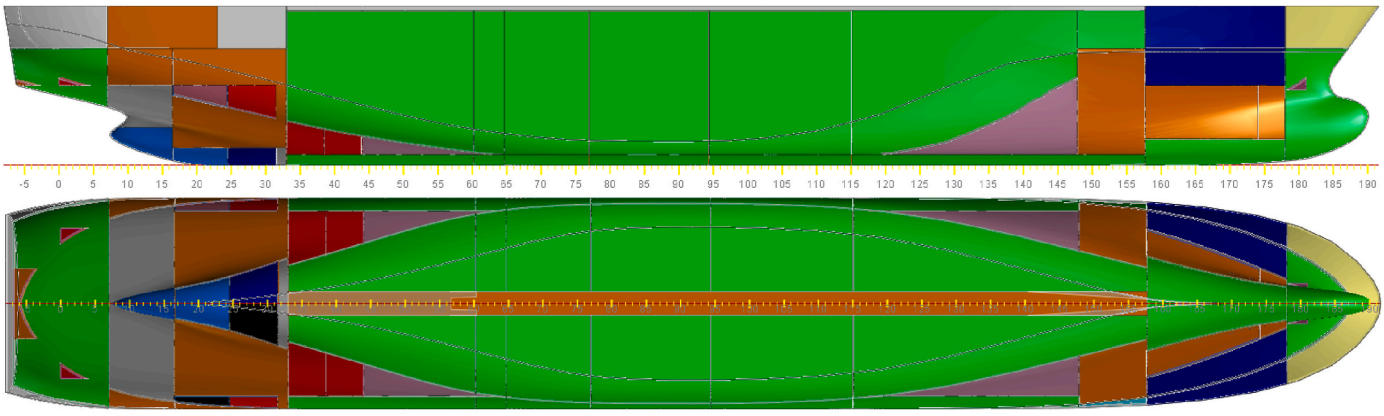

(a) Lowest Attained index of 0.513 with a corresponding cargo hold volume of 11,013 m^3

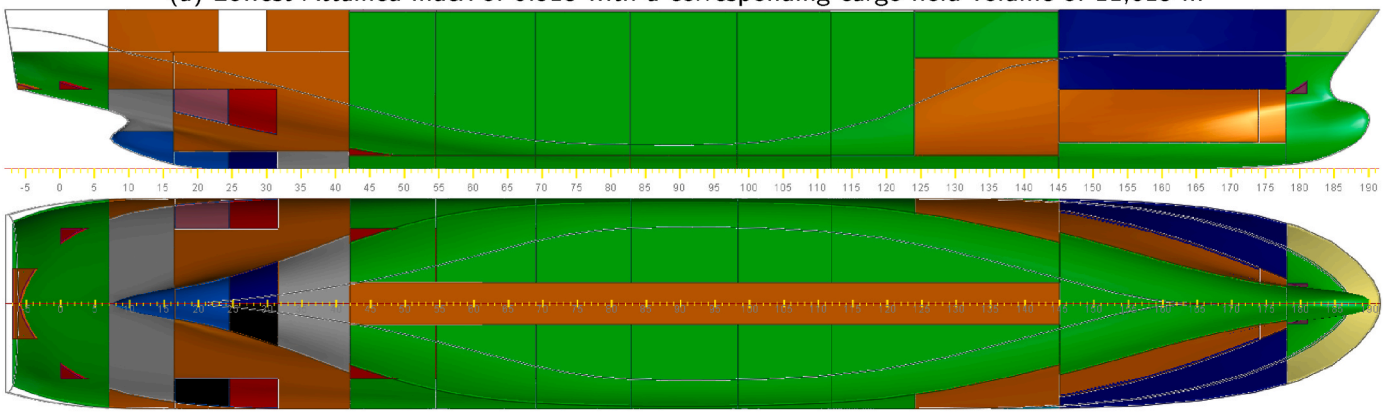

(b) Highest Attained index of 0.881 with a corresponding cargo hold volume of 6,612 m^3

Fig. 11. Extremities of the Pareto front for five water ballast bulkheads.

and only the last three parameters show reliable results.

The non-linear/non-monotonic behaviour of most of the parameters make it a complex task to determine what level of influence they actually have on the PDS and the parametric model. For instance, it was expected that the openings had a significant influence on the attained index. However, its elementary effect value is only marginal compared to the other parameters. To better understand the level of influence, more detailed analyses are needed to expand on the current findings, as the Morris method itself does not show a graph with the behaviour of the attained index over all trajectories. To generate more insight in the behaviour of the parameters and to strengthen the confidence in the results, a second analysis is performed.

6.2. Pearson correlation matrix

Another method of visualising the large numbers of data as a results from the optimisation method is the use of the Pearson correlation coefficient (Pearson, 1896). In this case, the input and output of the multi-objective optimisation is used as input to calculate the Pearson correlation coefficients. Especially for models with costly function evaluations like the PDS calculation, post-processing methods like this can be implemented relatively quick. The correlation matrix is comprised of Pearson correlation coefficients $r_{X,Y}$. These coefficients can be calculated using Eq. (10).

$$r_{X,Y} = \frac{\sum_{m}^{i=1}(X_i - \bar{X})(Y_i - \bar{Y})}{\sqrt{\sum_{m}^{i=1}(X_i - \bar{X})^2}\sqrt{\sum_{m}^{i=1}(Y_i - \bar{Y})^2}} \tag{10}$$

where X and Y are the two instances composed by m attributes and $\bar{X}$ and $\bar{Y}$ are defined using Eqs. (11) and (12):

$$\bar{X} = \frac{1}{m}\sum_{m}^{i=1} X_i \tag{11}$$

$$\bar{Y} = \frac{1}{m}\sum_{m}^{i=1} Y_i \tag{12}$$

The Pearson correlation coefficient shows the linear correlation between two variables. $r_{X,Y}$ ranges from -1 to 1, or from a strong negative to a strong positive correlation. Zero means that two variables are uncorrelated (Kijsipongse et al., 2011). All these values are combined into a symmetric $n \times n$ matrix, where n is the number of instances.

Fig. 15 shows the correlation matrix consisting of the Pearson correlation coefficients for the objectives, constraints and the five most influential parameters according to the Morris method results from Section 6.1. From these results, conclusions are drawn about the behaviour of the parameters:

Pump room - The size of the pump room has a positive correlation with the attained index, which means that for a high attained index, the pump room volume should become high as well. This can be seen in the coordinate plots in Fig. 12(a) and (b), where the size of the pump room increased between the lowest and highest attained index designs. The transverse bulkhead and deck of the pump room also show a similar correlation. The transverse bulkhead also shows high correlation with many of the other parameters. This is because it significantly influences both objectives, resulting in other parameters adjusting to its position. This phenomenon can be seen for all variables that have a high influence

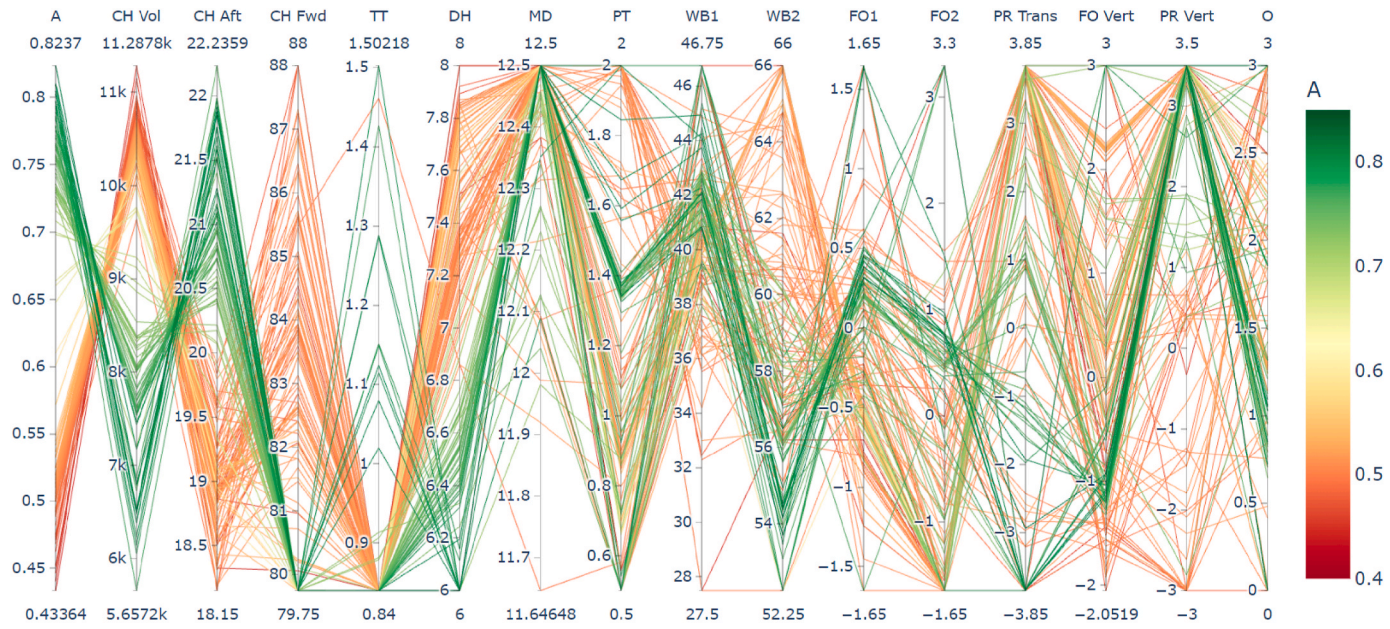

(a) Parallel coordinate plot for 200 iterations and two WB BH

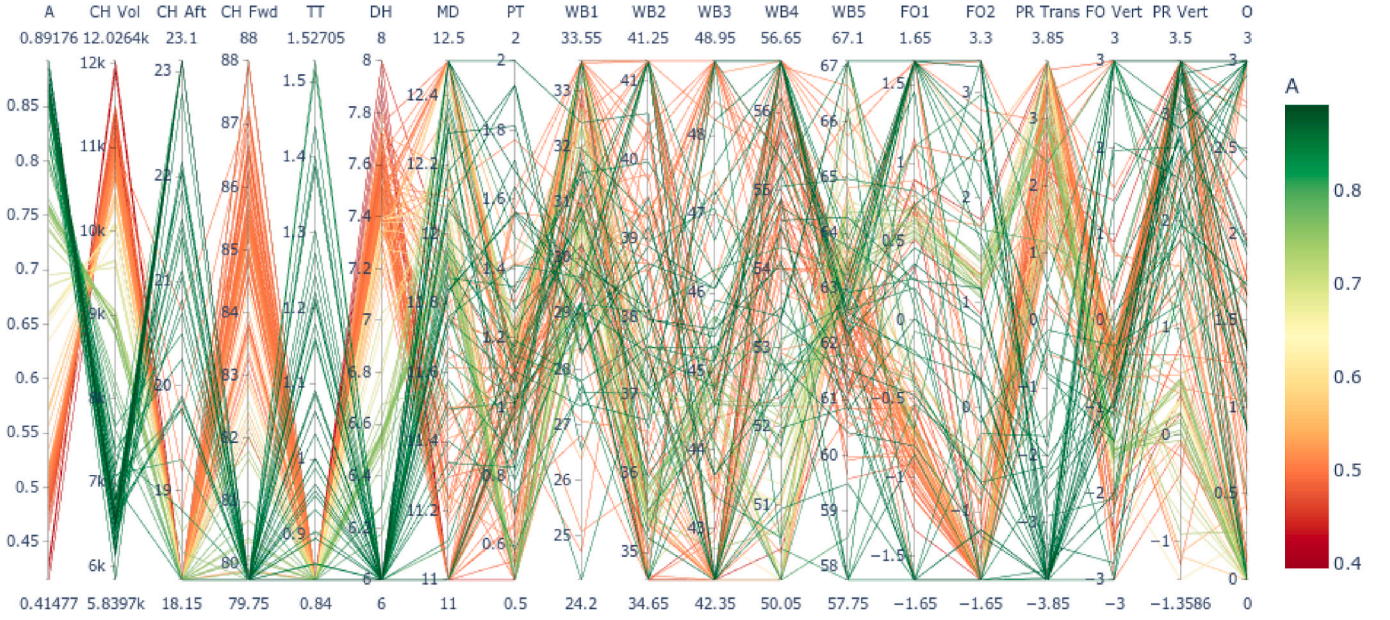

(b) Parallel coordinate plot for 200 iterations and five WB BH

Fig. 12. These figures show the objectives and parameter output as a result of the optimisation.

on one or both objectives. A particularly interesting result is the high correlation of the fourth water ballast bulkhead with both the pump room deck and the openings. The strong positive correlation means that the more the bulkhead is located forward, the higher the deck and openings tend to be located. This also goes the other way around, which is more likely as the influence of the water ballast bulkheads on the attained index is very low.

FO tanks - The FO tanks both have a negative correlation with the attained index. It can be seen that between the different designs, the fuel tanks remain relatively small compared to the increase in size of the pump room. The two transverse bulkheads and deck of the FO tanks show a marginal correlation between them and the attained index. If the size of the tanks do not matter, the two slightly different optimisation methods may show different FO tank designs that both have the same level of influence on the attained index. Both transverse bulkheads also show a strong correlation with the double hull and forward cargo hold bulkhead. This can be contributed to the fact that they all determine the size of the cargo hold, therefore depending on each other to determine this size, while maintaining a high attained index.

Water ballast bulkheads - As discussed above, the 4th and 5th water ballast bulkheads appear to have a high correlation with both the pump room and FO bulkheads respectively. As the water ballast

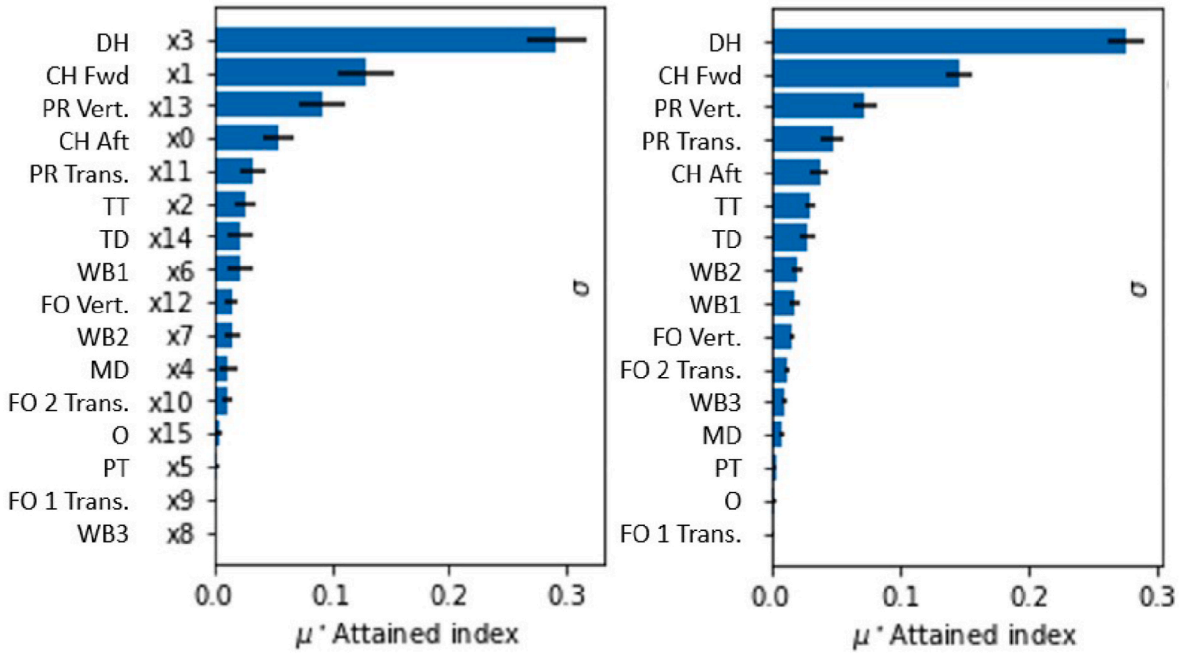

Fig. 13. Results of the Morris method for N = 20 and 100 respectively.

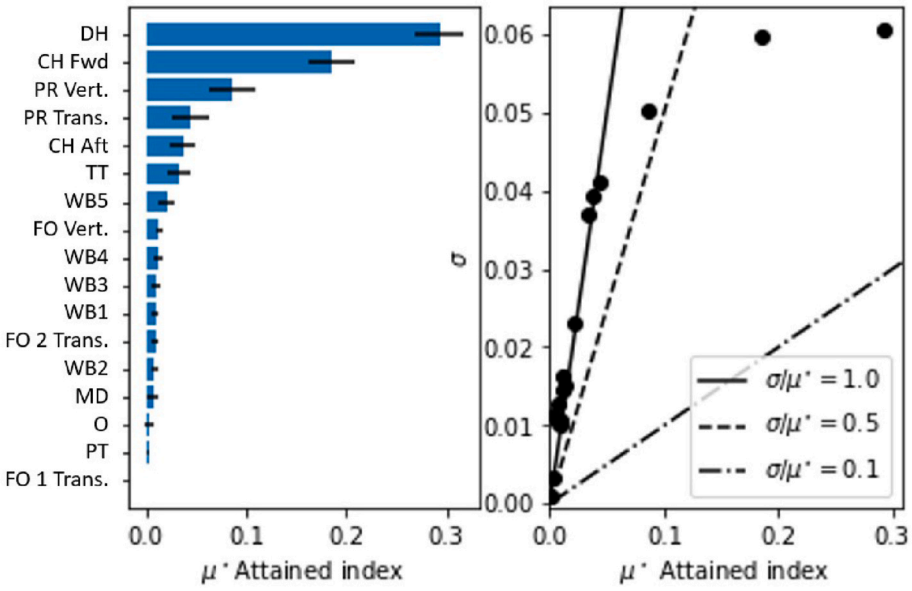

Fig. 14. Results of the Morris sensitivity analysis method of the second optimisation stage for five bulkheads.

bulkheads do not show a significant correlation with the attained index, it can be assumed that they are being influenced by the pump room and FO tanks instead of the other way around.

Cargo hold main bulkheads/decks - The main bulkheads are the cargo hold aft, forward and double hull bulkheads and the tanktop. These define the shape of the cargo hold, where the FO tanks and pump room are located. The difference in correlation for the cargo hold aft and forward bulkheads is discussed in Section 5, which verifies the difference between the two bulkheads. The longitudinal cargo hold bulkheads influences both the attained index and the cargo hold volume the most. Part of this reason is that the distance defined by the double hull defines the distance of both the PS and SB longitudinal cargo hold bulkhead. The tanktop correlation with the attained index and the cargo hold volume shows that it is much more important for the algorithm to maintain a low tanktop height as this greatly increases the cargo hold volume. That explains the reason the tanktop height remains minimum for all designs during this research. All main cargo hold bulkheads and decks have a high correlation with each other.

Main deck and openings - The main deck and openings are correlated as the height of the openings is semi-dependent on the main deck height. What stands out is that these two variables are not highly correlated. Their correlation is in the same vicinity as these variables have with many of the others. This could be attributed to the fact that after a certain height, the height of the openings has no influence on the attained index and the height of the openings becomes almost random from a certain point, lowering the correlation coefficient. Furthermore, these show a very low correlation with the attained index as their range is not sufficient enough to affect the attained index.

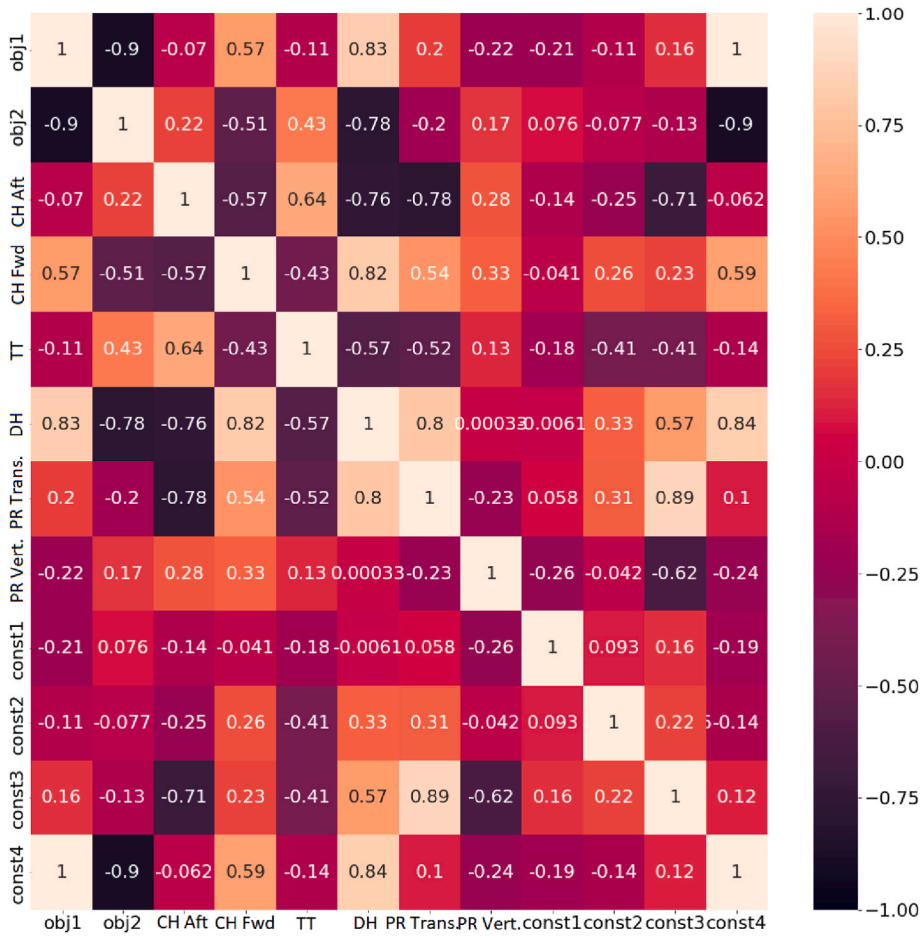

Fig. 15. Matrix containing all Pearson correlation coefficients for the objectives, constraints and the six most influential parameters according to the Morris method.

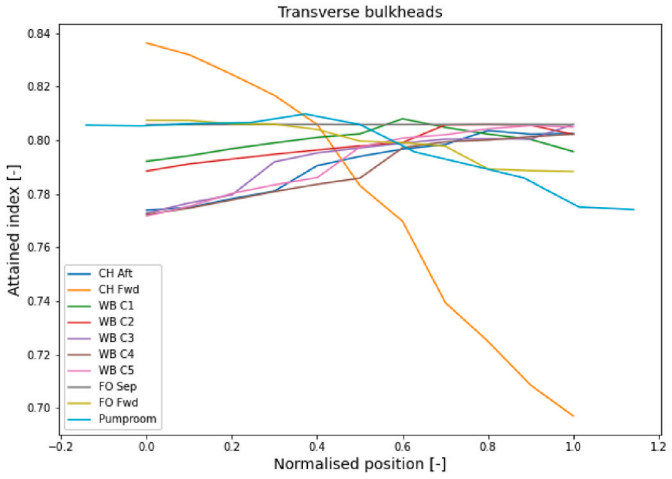

Fig. 16. Sensitivity in the normalised range of the transverse bulkheads with respect to the attained index A.

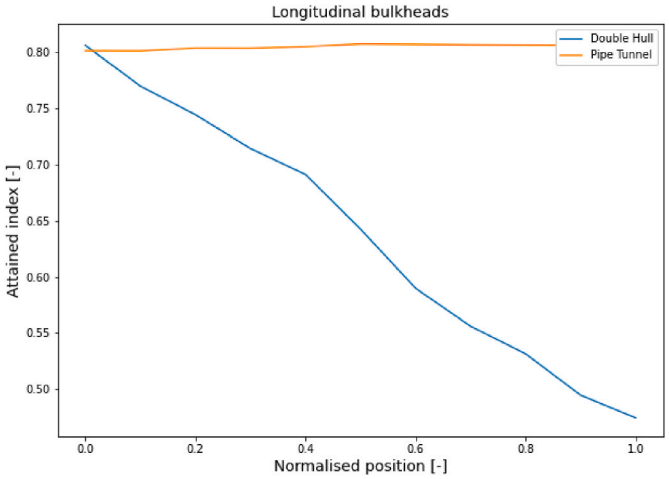

Fig. 17. Sensitivity in the normalised range of the longitudinal bulkheads with respect to the attained index A.

6.3. Manual local analysis

As both sensitivity analyses presented in this section lack clear, unambiguous answers to the parameter study, a final verification is performed to connect the two analyses with the research, each other, and the optimisation. This final verification is derived from a heuristic procedure proposed by Simopoulos et al. (2008), where the parameters behaviour is examined by manually changing one variable at a time, for which its value is determined by a certain interval, according to Eq. (13):

$$P_{i,j} = \frac{UB_i - LB_i}{x} \cdot y_j \tag{13}$$

where:

$P_{i,j}$ = ith parameter with the jth position in the interval;
UB_i= Upper boundary of the ith parameter;
LB_i = Lower boundary of the ith parameter;

x = Number of intervals as an integer;
y_j = Position in the interval as an integer.

The base ship is used as a starting point, where all variable values return to if they are not subjected to change. The number of function evaluations for this sensitivity analysis is $x + 1$ times the number of variables. This means that 176 function evaluations are necessary for this case study to obtain the results. The results are normalised and combined into three groups of graphs representing the behaviour of the transverse, longitudinal, and vertical location of the parameters respectively. The range is normalised to show the relative influence of the parameters with respect to their total allowable range.

Fig. 16 shows that most variables have the same level of influence on the attained index. They do not change the attained index by approximately more than 5% over their entire range. However, the transverse bulkhead that represents the front of the cargo hold shows a significantly higher influence. With the attained index dropping from 0.84 to 0.70, a difference of 0.14 in attained index is recorded between this variable's lower and upper boundary. The more the bulkhead is positioned to the aft of the ship, the higher the attained index becomes. However, this also reduces the size of the cargo hold significantly. This supports and strengthens the results described in Chapter 5 and the correlation matrix results of Section 6.2, where the forward cargo hold bulkhead also showed the same behaviour. This also applies to the pump room bulkhead that has a strong negative correlation with the attained index, and the water ballast bulkheads that converge to equal spacing for the same reason.

Only two longitudinal bulkheads are located in the middle section. The difference in influence by these two variables is visible in Fig. 17. The pipe tunnel is located in the centre of the double bottom. The range of the pipe tunnel is relatively small and does not extend far from the centreline of the ship (0.5–2 m). An increase in breadth of the pipe tunnel does not influence many new damage cases as the penetration depth of the damages do simply not reach the tunnel. The inside of the double hull changes the size of the cargo hold and distance from the side shell significantly (6–8 m), which results in a relatively large influence on the attained index.

The level of influence on the attained index is relatively the same for the decks and openings. However, some particularities can be observed from Fig. 18. The height of the openings shows a relatively large influence in the first quarter of its range until the openings are located above the damaged waterline. The height of the FO bunker tank only negatively influences the attained index the higher it becomes. This is in contrast to the height of the pump room, where an increase in height seems to exponentially influence the attained survivability index.

The sensitivity analysis by hand discussed in this section only shows the influence of the parameters concerning the base ship model. This is therefore not a global analysis that results in the sensitivity of the parameters over the entire parameter space. However, as the base ship model is realistic, it does show the behaviour of the parameters in the vicinity of a reasonably optimised model. Combined with the post-processing Pearson correlation matrix and the Morris sensitivity analysis, the optimisation can be validated and insight into the PDS calculation is generated.

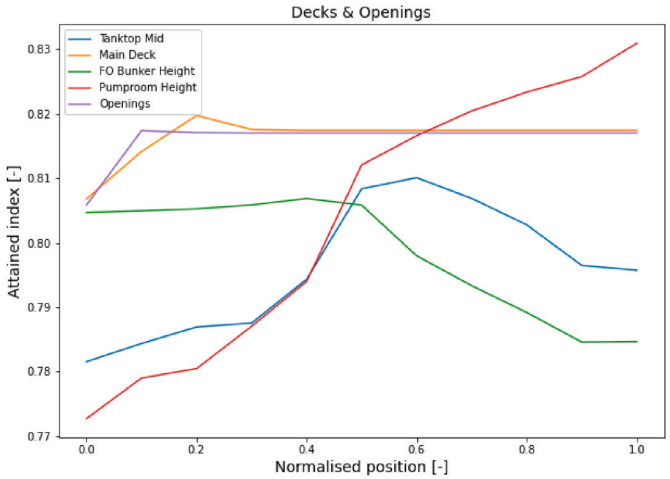

Fig. 18. Sensitivity in the normalised range of the decks and openings concerning the attained index A.

7. Conclusions

This paper proposed a new framework for damage stability for use early in the design process. The framework incorporates both a multi-level global optimisation algorithm and a global sensitivity analysis method that aims at providing a preliminary design while elucidating the level of influence of the parameters respectively. One of the aims of the study was to generate a generic framework in order to extend the applicability of the research from the current case study to single hold ships in general. The multi-level optimisation showed good results in proposing a set of preliminary designs. These designs showed interesting trends with respect to the decisions made within the framework. Results showed that the highest priority for single hold ships is the protection of the cargo hold. However, the methods used within the framework to reach this goal provide unique insight in the early stages of design.

The advantage of the optimisation algorithm proposed within the framework is that it fully explores the parameter space, creating far more designs than the designer is able to generate in the same amount of time. This way, the chances of finding more fitting and innovative designs increases significantly. This is especially useful as there are numerous methods to, for instance, create more distance between the cargo hold and the hull. These methods can be implemented in the optimisation method and their influence on the design is then provided.

The sensitivity analysis results provided by the Morris method showed that the parameters behaved mostly non-linear and non-monotonic and were therefore difficult to distinguish when looking at their influence on the attained index. The use of the correlation matrix and the verification by hand provided the rest of the insight obtained from the research. In the end, the sensitivity analysis explained and validated the decisions made within the framework and provided some interesting insight in the characteristics of the parameters and the compartments that were assigned to them. The influence of the parameters was measured over their respective boundaries. These boundaries were chosen such that they represented realistic locations in an actual ship design. This greatly influenced the level of influence these parameters had on the design. However, as this research is performed from the perspective of the designer, this is exactly the type of influence that is aimed for. Therefore, all results for the sensitivity analyses are normalised. Listed below are the general findings from the sensitivity analysis.

- Most parameters behave non-linear/non-monotonic,
- Influence of parameters on the attained index can be distorted by their respective boundaries,
- Morris method is therefore only reliable for most influential variables,
- The correlation matrix can be useful, but should always be evaluated critically by the designers,
- The combination of different sensitivity analysis methods together with an optimisation method, provides significant insight in the behaviour of the PDS calculation.

The following behaviour of the multi-objective optimisation method is validated and further insight is given by the sensitivity analyses:

- Forward cargo hold bulkhead has a higher influence than the aft bulkhead due to its respective distance from the hull,

- Openings and main deck do not significantly influence the attained index in their current boundaries, but do so beyond these boundaries,
- Even though the number of water ballast bulkheads has a lot of influence on the attained index, their location, within their respective boundaries, does not,
- A higher pump room volume results in a higher attained index,
- The shape of the FO tanks is not important to the attained index.

The limitations that can be found in this research are both general limitations for optimisation problems and sensitivity analysis models as well as research specific limitations. A limitation of the optimisation algorithm can be found in the limited number of parameters that can be chosen. Even though the algorithm used is capable of handling relatively many parameters, it is not possible to create a holistic model that handles every single parameter that influences the damage stability of a ship design. The limitations of the sensitivity analyses mainly originate from the nature of the non-linear results.

8. Future work

To further expand this research, the actual weight change per iteration and therefore change in GM can be added in the first optimisation stage. The accuracy of the results would also increase from varying the GM with the height of the different decks. Also the increase in draught due to a higher main deck can be used as a dependent variable to increase the accuracy of the research even more. Multi-threading can be used to speed up the optimisation and another global sensitivity analysis can be used which is better at dealing with non-linear parameters.

As was stated in Section 1, the freedom potential offered by the PDS regulations to use them as a base of design is difficult to capitalise on when it is unclear what the behaviour of- and coherence between the parameters is. By providing an optimised preliminary design and insight in this behaviour and coherence, the design freedom that comes with the PDS regulations can now be better explored. Ship designers can use the framework as a base of design and can continue using it in later stages as well, when, due to other design requirements, the design does not satisfy the required index anymore.

In this paper, only the middle section of the ship is used as a case study. It is however, up to the designer to decide which parameters are selected. An even smaller section of the ship can be investigated in greater detail, or parameters over the entire length can be used for a more high level investigation. The use of the framework is also not limited to cargo ships and can be used on all types of ships that are subjected to the PDS regulations.

Declaration of competing interest

The authors declare that they have no known competing financial interests or personal relationships that could have appeared to influence the work reported in this paper.

Acknowledgements

This work was performed at Delft University of Technology in the Netherlands as part of an academic thesis (Milatz, 2022), and thus, there was no real funding sponsor involved. The contributing entities are those listed in the text (Delft University of Technology, C-Job Naval Architects, and DELFTship Maritime Software).

References

Alarie, S., Audet, C., Gheribi, A.E., Kokkolaras, M., Le Digabel, S., 2021. Two decades of blackbox optimization applications. EURO J. Comput. Optim. 9 https://doi.org/10.1016/j.ejco.2021.100011.

Andrews, D., Dicks, C., 1997. The building block design methodology applied to advanced naval ship design. In: Proceedings of the 6Th International Marine Design Conference, IMDC'97. Newcastle-upon-Tyne, UK, pp. 3–19.

Beume, N., Naujoks, B., Emmerich, M., 2007. SMS-EMOA: multiobjective selection based on dominated hypervolume. Eur. J. Oper. Res. 181, 1653–1669. https://doi.org/10.1016/j.ejor.2006.08.008.

Bossek, J., Doerr, C., Kerschke, P., 2020. Initial design strategies and their effects on sequential model-based optimization: an exploratory case study based on BBOB. In: GECCO 2020 - Proceedings of the 2020 Genetic and Evolutionary Computation Conference. Association for Computing Machinery, pp. 778–786. https://doi.org/10.1145/3377930.3390155.

Bulian, G., Cardinale, M., Dafermos, G., Eliopoulou, E., Francescutto, A., Hamann, R., Linderoth, D., Luhmann, H., Ruponen, P., Zaraphonitis, G., 2019. Considering collision, bottom grounding and side grounding/contact in a common non-zonal framework. In: 17th International Ship Stability Workshop.

Bulian, G., Lindroth, D., Ruponen, P., Zaraphonitis, G., 2016. Probabilistic assessment of damaged ship survivability in case of grounding: development of a direct non-zonal approach. Ocean Eng. 120, 331–338.

Campolongo, F., Cariboni, J., Saltelli, A., 2007. An effective screening design for sensitivity analysis of large models. Environ. Model. Software 22, 1509–1518. https://doi.org/10.1016/j.envsoft.2006.10.004.

Campolongo, F., Cariboni, J., Saltelli, A., Schoutens, W., 2005. Enhancing the Morris Method. Technical Report. European Commission, Joint Research Centre, Ispra. http://library.lanl.gov/.

Campolongo, F., Saltelli, A., 1997. Sensitivity Analysis of an Environmental Model: an Application of Different Analysis Methods. Technical Report. Faculty of Environmental Sciences, Griffith University, Nathan Campus, 4111 QLD, Australia. Environment Institute, Joint Research Centre, TP 272, 21020 Ispra (VA), Italy.

Campolongo, F., Tarantola, S., Saltelli, A., 1999. Tackling Quantitatively Large Dimensionality Problems. Institute for Systems, Informatics and Safety. Technical Report.

Conti, F., Le Sourne, H., Vassalos, D., Kujala, P., Lindroth, D., Kim, S., Hirdaris, S., 2021. A Comparative Method for Scaling Solas Collision Damage Distributions Based on a Ship Crashworthiness Application to Probabilistic Damage Analysis of a Passenger Ship. Ship and Offshore Structures in press.

DELFTship Maritime Software, 2022. DELFTship: Visual Hull Modelling and Stability Analysis. https://www.delftship.net/.

eSAFE, 2017-2018. Enhanced Stability after a Flooding Event. A Joint Industry Project on Damage Stability for Cruise Ships.

FLARE, 2018-2022. Flooding Accident Response. EU Funded Research Project, Contract No, 814753. www.flare-project.eu.

GOALDS, 2009-2012. Goal Based Damage Stability. EU-funded FP7 project.

Halton, J.H., 1960. On the efficiency of certain quasi-random sequences of points in evaluating multi-dimensional integrals. Technical Report. Numer. Math. 2.

HARDER, 2000-2003. Harmonization of Rules and Design Rational. EU Funded Research Project, FP5, DG XII-BRITE.

Herman, J., Kollat, J., Reed, P., Wagener, T., 2013. Method of Morris effectively reduces the computational demands of global sensitivity analysis for distributed watershed models. Hydrol. Earth Syst. Sci. 17, 2893–2903.

Herman, J., Usher, W., 2017. SALib: an open-source Python library for Sensitivity Analysis. J. Open Source Softw. 97.

IMO, 2009. SOLAS-international Convention for the Safety of Life at Sea (SOLAS). Technical Report. International Maritime Organisation, London, UK.

IMO, 2020a. Chapter II-1 - Construction - Structure, Subdivision and Stability, Machinery and Electrical Installations, Part B - Subdivision and Stability. International Maritime Organization. Technical Report.

IMO, 2020b. SOLAS-international Convention for the Safety of Life at Sea (SOLAS). Technical Report. International Maritime Organisation. Consolidated edition as of 2020.

Kijsipongse, E., U-Ruekolan, S., Ngamphiw, C., Tongsima, S., 2011. Efficient large Pearson correlation matrix computing using hybrid MPI/CUDA. In: Proceedings of the 2011 8th International Joint Conference on Computer Science and Software Engineering. JCSSE, pp. 237–241. https://doi.org/10.1109/JCSSE.2011.5930127, 2011.

Koelman, H.J., Pinkster, J., 2003. Rationalizing the Practice of Probabilistic Damage Stability Calculations. Technical University Delft, Department of Marine Technology Ship Hydrodynamics Laboratory. Technical Report 3.

Krüger, S., 2023. Statutory and operational damage stability by a Monte Carlo based approach. J. Mar. Sci. Eng. 11, 16.

Krüger, S., Dankowski, H., 2019. A Monte Carlo based simulation method for damage stability problems. In: ASME 2019 38th International Conference on Ocean. Offshore and Artic Engineering. OMAE 2019).

Krüger, S., Kehren, F., Dankowski, H., 2008. Leckstabilitätsberechnungen durch Monte Carlo simulationen. Festschrift, Schiftenreiche Shiffbau 641, 60–85. In German.

Lützen, M., 2014. Ship Collision Damage. Technical University of Denmark. Technical Report. https://www.researchgate.net/publication/264374677.

Manderbacka, T., Themelis, N., Bačkalov, I., Boulougouris, E., Eliopoulou, E., Hashimoto, H., Konovessis, D., Leguen, J., Miguez Gonzalez, M., Rodriguez, C., Rosen, A., Ruponen, P., 2019. An overview of the current research on stability of ships and ocean vehicles: the stab2018 perspective. Ocean Eng. 186, 106090.

MARPOL - International Convention for the Prevention of Polluition from Ships, 2007. Annex I - Regulation 12A - Oil Fuel Tank Protection. IMO.

Mauro, F., Braidotti, L., Trincas, G., 2019. A model for intact and damage stability evaluation of CNG ships during the concept design stage. J. Mar. Sci. Eng. 7 (12), 450.

Mauro, F., Vassalos, D., 2022. The influence of damage breach sampling process on the direct assessment of ship survivability. Ocean Eng. 250, 111008.
Mauro, F., Vassalos, D., Paterson, D., 2022. Critical damages identification in a multi-level damage stability assessment framework for passenger ships. Reliab. Eng. Syst. Saf. 228, 108802.
Mauro, F., Vassalos, D., Paterson, D., Boulougouris, E., 2023. Evolution of ship damage stability assessment—transitioning designers to direct numerical simulations. Ocean Eng. 268, 113387.
Milatz, B., 2022. Multi-level Optimisation and Global Sensitivity Analysis of the Probabilistic Damage Stability Method for Single Hold Ships. MSc Thesis, Delft University of Technology. http://resolver.tudelft.nl/uuid:24b94160-8804-4d9a-887f-24e3c68ae89c.
Morris, M.D., 1991. Factorial sampling plans for preliminary computational experiments. Technometrics 33, 161–174.
Naydenov, L., Georgiev, P., 2013. Probabilistic analysis of damage stability of ships based on metamodels. In: Proceedings of IMAM 2013, pp. 769–777.
Papanikolaou, A., 2007. Review of damage stability of ships - recent developments and trends. In: 10th International Symposium on Practical Design of Ships and Other Floating Structures. PRADS, pp. 497–509, 2007.
Papanikolaou, A., Hamman, R., Lee, B., Mains, C., Olufsen, O., Vassalos, D., Zaraphonitis, G., 2013. Goalds: goal based damage ship stability and safety standards. Accid. Anal. Prev. 60, 353–365.
Pawlowski, M., 2004. Subdivision and Damaged Stability of Ships. Euro-MTEC book series, Gdansk, Poland.
Pearson, K., 1896. Mathematical contributions to the theory of evolution.—III. Regression, heredity and panmixia. Philos. Trans. R. Soc. London, A 187, 253–318.
Powell, M.J.D., 1994. A direct search optimization method that models the objective and constraint functions by linear interpolation. In: Advances in Optimization and Numerical Analysis. Springer, Netherlands, pp. 51–67.
Ruponen, P., Lindroth, D., Routi, A., Aartovaara, M., 2019. Simulation-based analysis method for damage survivability of passenger ships. Ship Technol. Res. 66, 180–192.
Ruponen, P., Valanto, P., Acanfora, M., Dankowski, H., Lee, G., Mauro, F., Murphy, A., Rosano, G., van't Veer, R., 2022. Results of an international benchmark study on numerical simulation of flooding and motions of a damaged ropax ship. Appl. Ocean Res. 123, 103153.
Saltelli, A., Tarantola, S., Campolongo, F., Ratto, M., 2004. Sensitivity Analysis in Practice : A Guide to Assessing Scientific Models. John Wiley & Sons.
Simopoulos, G., Konovessis, D., Vassalos, D., 2008. Sensitivity analysis of the probabilistic damage stability regulations for RoPax vessels. J. Mar. Sci. Technol. 13, 164–177. https://doi.org/10.1007/s00773-007-0261-x.
Spanos, D., Papanikolaou, A., 2014. On the time for abandonement of flooded passenger shipsdue to collision damages. J. Mar. Sci. Technol. 19, 327–337.
Tuzcu, C., 2003. Development of the factor-s: the damage survival probability. In: 8th International Conference on the Stability of Ships and Ocean Vehicles.
Vassalos, D., 2022. The role of damaged ship dynamics in addressing the risk of flooding. Ships Offshore Struct. 17, 279–303.
Vassalos, D., Guarin, L., 2009. Designing for damage stability and survivability–contemporary developments and implementation. Ship Sci. Technol. 5 (1), 57–69.
Vassalos, D., Paterson, D., Mauro, F., Atzampos, G., Assinder, P., Janicek, A., 2022a. Critical damages identification in a multi-level damage stability assessment framework for passenger ships. Appl. Sci. 12, 4949.
Vassalos, D., Paterson, D., Mauro, F., Mujeeb-Ahmed, M., Boulougouris, E., 2022b. Process, methods and tools for ship damage stability and flooding risk assessment. Ocean Eng. 266, 113062.
Vassalos, D., York, A., Jasionowski, A., Kanerva, M., Scott, A., 2007. Design Implications of the New Harmonised Probabilistic Damage Stability Regulations. Technical Report.
de Winter, R., Bronkhorst, P., van Stein, B., Bäck, T., 2022. Constrained multi-objective optimization with a limited budget of function evaluations. Memetic Comput. 14, 151–164.
de Winter, R., van Stein, B., Bäck, T., 2021. SAMO-COBRA: a fast surrogate assisted constrained multi-objective optimization algorithm. In: Lecture Notes in Computer Science (Including Subseries Lecture Notes in Artificial Intelligence and Lecture Notes in Bioinformatics). Springer Science and Business Media Deutschland GmbH, pp. 270–282. https://doi.org/10.1007/978-3-030-72062-9_22.
Zang, M., Conti, F., Le Sourne, H., Vassalos, D., Kujala, P., Lindroth, D., Hirdaris, S., 2021. A method for the direct assessment of ship collision damage and flooding risk in real conditions. Ocean Eng. 237, 109605.
Zitzler, E., Thiele, L., 1998. Multiobjective optimization using evolutionary algorithms—a comparative case study. In: Eiben, A.E., Bäck, T., Schoenauer, M., Schwefel, H.P. (Eds.), International Conference on Parallel Problem Solving from Nature (PPSN). Springer, pp. 292–301.